

University of Groningen

Aquatic vertebrate locomotion

Videler, JJ; Muller, UK; Stamhuis, EJ

Published in:
Journal of Experimental Biology

IMPORTANT NOTE: You are advised to consult the publisher's version (publisher's PDF) if you wish to cite from it. Please check the document version below.

Document Version
Publisher's PDF, also known as Version of record

Publication date:
1999

[Link to publication in University of Groningen/UMCG research database](#)

Citation for published version (APA):

Videler, JJ., Muller, UK., & Stamhuis, EJ. (1999). Aquatic vertebrate locomotion: Wakes from body waves. *Journal of Experimental Biology*, 202(23), 3423-3430.

Copyright

Other than for strictly personal use, it is not permitted to download or to forward/distribute the text or part of it without the consent of the author(s) and/or copyright holder(s), unless the work is under an open content license (like Creative Commons).

Take-down policy

If you believe that this document breaches copyright please contact us providing details, and we will remove access to the work immediately and investigate your claim.

Downloaded from the University of Groningen/UMCG research database (Pure): <http://www.rug.nl/research/portal>. For technical reasons the number of authors shown on this cover page is limited to 10 maximum.

AQUATIC VERTEBRATE LOCOMOTION: WAKES FROM BODY WAVES

J. J. VIDELER*, U. K. MÜLLER AND E. J. STAMHUIS

Department of Marine Biology, Groningen University, The Netherlands

*e-mail: j.j.videler@biol.rug.nl

Accepted 29 July; published on WWW 16 November 1999

Summary

Vertebrates swimming with undulations of the body and tail have inflection points where the curvature of the body changes from concave to convex or *vice versa*. These inflection points travel down the body at the speed of the running wave of bending. In movements with increasing amplitudes, the body rotates around the inflection points, inducing semicircular flows in the adjacent water on both sides of the body that together form proto-vortices. Like the inflection points, the proto-vortices travel towards the end of the tail. In the experiments described here, the phase relationship between the tailbeat cycle and the inflection point cycle can be used as a first approximation of the phase between the proto-vortex and the tailbeat cycle. Proto-vortices are shed at the tail as body vortices at roughly the same time as the inflection points reach the tail tip. Thus, the phase between proto-vortex shedding and tailbeat cycle determines the interaction between body and tail vortices,

which are shed when the tail changes direction. The shape of the body wave is under the control of the fish and determines the position of vortex shedding relative to the mean path of motion. This, in turn, determines whether and how the body vortex interacts with the tail vortex. The shape of the wake and the contribution of the body to thrust depend on this interaction between body vortex and tail vortex. So far, we have been able to describe two types of wake. One has two vortices per tailbeat where each vortex consists of a tail vortex enhanced by a body vortex. A second, more variable, type of wake has four vortices per tailbeat: two tail vortices and two body vortices shed from the tail tip while it is moving from one extreme position to the next. The function of the second type is still enigmatic.

Key words: locomotion, body wave, wake, vertebrate, swimming, vortex.

Introduction

Many aquatic vertebrates swim by means of waves of curvature running down their elongated body. Most fish undulate from side to side in a horizontal plane. Flatfish and cetaceans move their body and tail vertically. During undulatory swimming, waves run from head to tail with increasing amplitude. The interaction between the undulating body and the water results in flow patterns along and behind the swimming animal. Here, we are interested in fundamental aspects of the morphology of the flow caused by undulatory propulsion during steady, straight, forward swimming at close to uniform velocities.

Hydrodynamic theory has been used to predict the thrust and the wake generated by undulatory swimmers (Aleyev, 1977; Lighthill, 1975). Hydrodynamic approaches usually focus on the flow generated by the tail. The body undulations are considered to drive the tail motion rather than to contribute significantly to the thrust (Lighthill, 1970). Therefore, the influence of the body on the flow is either ignored or even considered to be detrimental, because the lateral body excursions might increase the drag relative to that of a straight body. A schematic three-dimensional impression of the wake behind a fish is shown in Fig. 1 (Videler, 1993). It shows the dorsal and ventral tip vortices generated by the tail during the

tailbeat as well as the vertical stop–start vortices left behind by the trailing edge of the tail at the end of each half-stroke. These vortex systems form a chain through which a jet of water undulates in the direction opposite to the swimming direction. We will restrict our discussion to what happens in a medio-frontal plane through the fish and the wake. In this plane, we expect to see left and right stop–start vortices with an undulating backward jet between them. The rotational sense should be anticlockwise on the right of the fish and clockwise on the left. Visualisations of the flow in the medio-frontal plane of swimming fish should reveal whether this picture of the wake is correct.

Early qualitative attempts to visualise the motions of the fluid provided an overall impression of the flow patterns without clear directional information. Gray (1968) photographed an eel (*Anguilla anguilla*) swimming through water seeded with small polyethylene particles (Fig. 2). The flow pattern in the wake shown by the blurred particles resembles a vortex street consistent with theoretical predictions. The picture also suggests that vortical flow patterns are not restricted to the wake. The water adjacent to the undulating body moves along curved paths. Hertel (1966) observed the movements of particles in the flow around a water

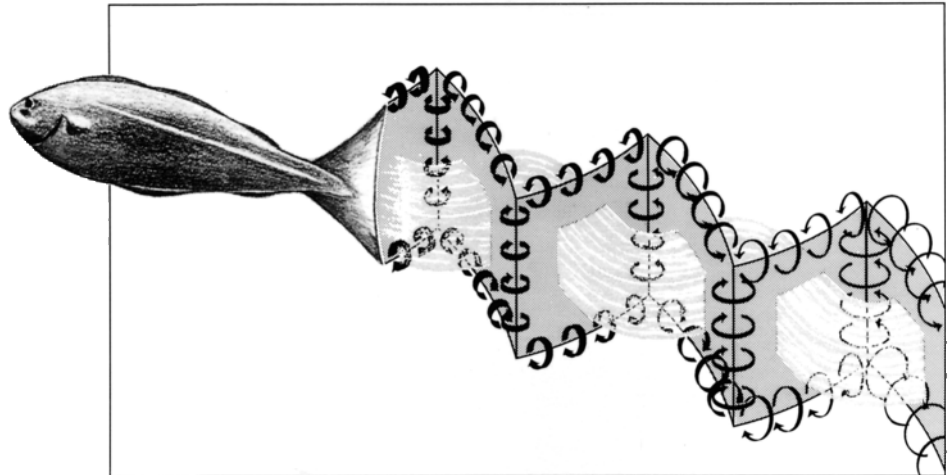


Fig. 1. An impression of the three-dimensional vortex flow system and the resulting jet behind a steadily swimming saithe. The impression is based on theoretical considerations and qualitative experimental evidence of the shape of the wake in a horizontal plane through the middle of the fish (taken from Videler, 1993, with permission).

snake (*Natrix natrix*) swimming near the surface and observed the same semicircular currents on both sides along the undulating body. Rosen (1959) visualised the wake below a pearl danio (*Brachidanio albolineatus*) using a layer of milk. In the wake of the fish, he observed a single row of large vortices close to the mean path of motion and small vortices on either side of the large ones (Fig. 3A). This wake pattern is not consistent with theoretical predictions. The fish also appears to generate separation vortices along the body. Rosen's (1959) solid peg theory was the first attempt to interpret body flows as useful for the generation of thrust. However, vortices do not behave like solid pegs, and Rosen's interpretation of thrust generation must be considered flawed.

Several questions remain. Which wake pattern is typical of undulatory swimmers? How are wake patterns generated? What is the role of the undulating body in the production of wake patterns? Does the body contribute to the generation of thrust? Recent experiments combine quantitative hydrodynamic and kinematic studies to compare the movements of the fish directly with the resulting flow patterns (Müller et al., 1997; Müller, 1997). These experiments should help in answering the questions raised.

Wakes behind undulatory swimmers

Particle image velocimetry allows quantitative measurements of both the direction and speed of the flow (Stamhuis and Videler, 1995). This technique was employed to describe the wakes of a mullet (*Chelon labrosus*) (Müller et al., 1997) and an eel (Müller, 1997), both swimming continuously along a straight path. The wake behind a steadily swimming mullet is shown in Fig. 4 (taken from Müller et al., 1997). The black arrows indicate the flow velocity and the

coloured squares the level of vorticity in the flow. The filled blue shadowgraph and the blue outline on the far left of the figure show the tail of the fish just before it leaves the field of view. The time span between shadowgraph and outline is

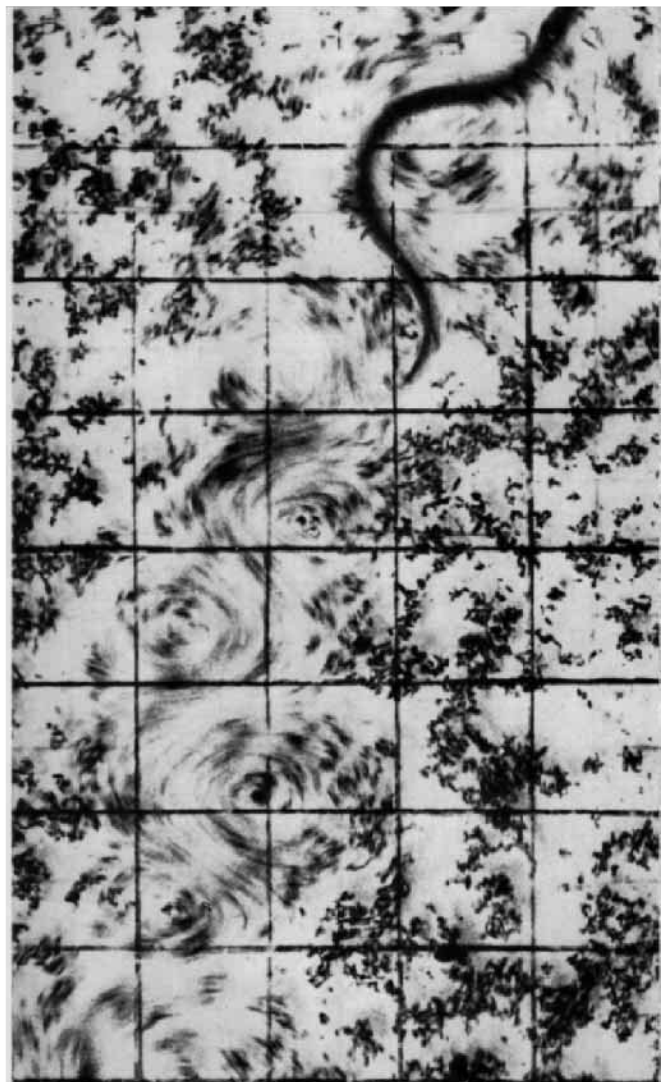


Fig. 2. Vortices formed near a 16cm long eel swimming in a suspension of polyethylene particles at a speed of approximately 9 cm s^{-1} . The propulsive wave runs down the body at 15 cm s^{-1} . The tailbeat frequency is 1.7 Hz (taken from Gray, 1968, with permission).

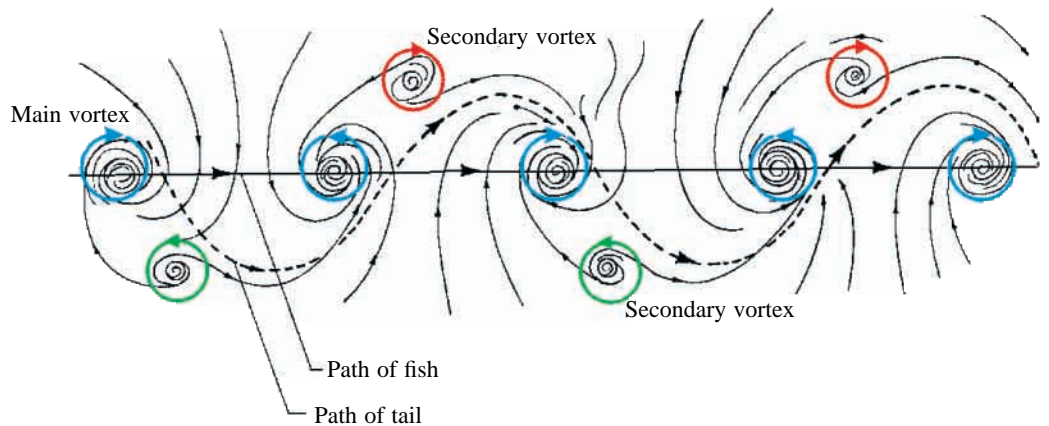
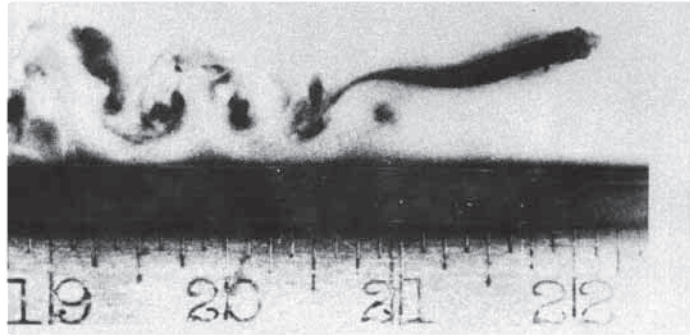


Fig. 3. (A) The flow in the wake of a pearl danio visualised with a layer of milk just below the swimming fish (taken from Rosen, 1959, with permission). (B) Rosen's (1959) interpretation of the wake. The coloured circular arrows indicate the rotational sense of the vortices on the basis of the current analysis of the wakes generated by undulatory swimmers.

0.04 s. In a medio-frontal plane, the undulatory swimming movements of the mullet create a wake resembling the vortex street observed by Gray (1968). The flow field behind an 8 cm eel is depicted in Fig. 5 (taken from Müller, 1997). The eel sheds a wake very similar to the pearl danio of Rosen (1959) with two vortices shed per half-tailbeat.

Eels can obviously generate at least two wake patterns with a body wave amplitude increasing almost linearly from head to tail. Mullet and pearl danio have a similar fusiform shape, and the amplitude envelope of their body waves has the shape of a power function. Still, their wakes are very different.

Flow adjacent to the body of undulatory swimmers

Despite the obvious differences in their respective wakes, mullet (Fig. 6) and eel (Fig. 7) create the same semicircular flow patterns on their body as previously observed by Gray (1968) and Hertel (1966). The mechanism of flow production is related to the undulatory movement of the body. The lateral displacements of the body seem to create low-pressure areas

near concave body zones and high-pressure areas near convex body zones. The pressure differential along the body, together with the undulatory motion of the body, appears to induce semicircular flow patterns from the high- to the low-pressure areas. High- and low-pressure areas interchange along the body, and a low-pressure area on the concave side of the body is complemented by a high-pressure area on the opposite convex side of the body. The clockwise semicircular flow pattern on one side of the body is complemented by another

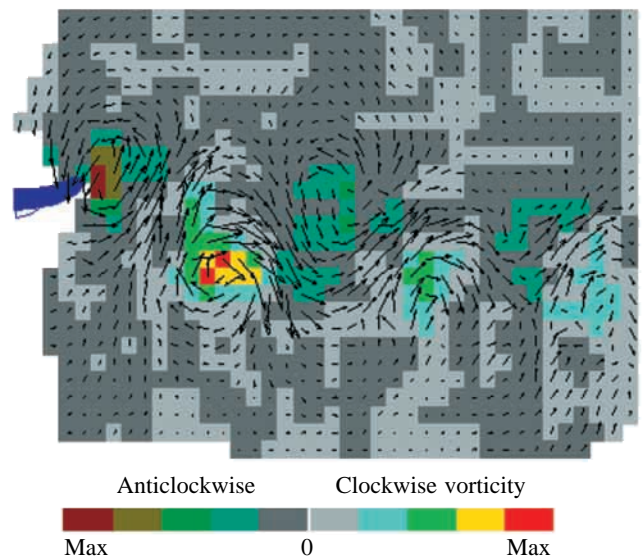


Fig. 4. The wake behind a 0.126 m long mullet swimming steadily at 0.175 m s^{-1} (taken from Müller et al., 1997). The arrows indicate the flow velocity, and the coloured squares indicate the strength of the vorticity. The fish has just left the field of view to the left. The wake consists of a zigzag row of vortices with two vortices shed per tailbeat cycle. An undulating jet separates the two rows of alternating vortices.

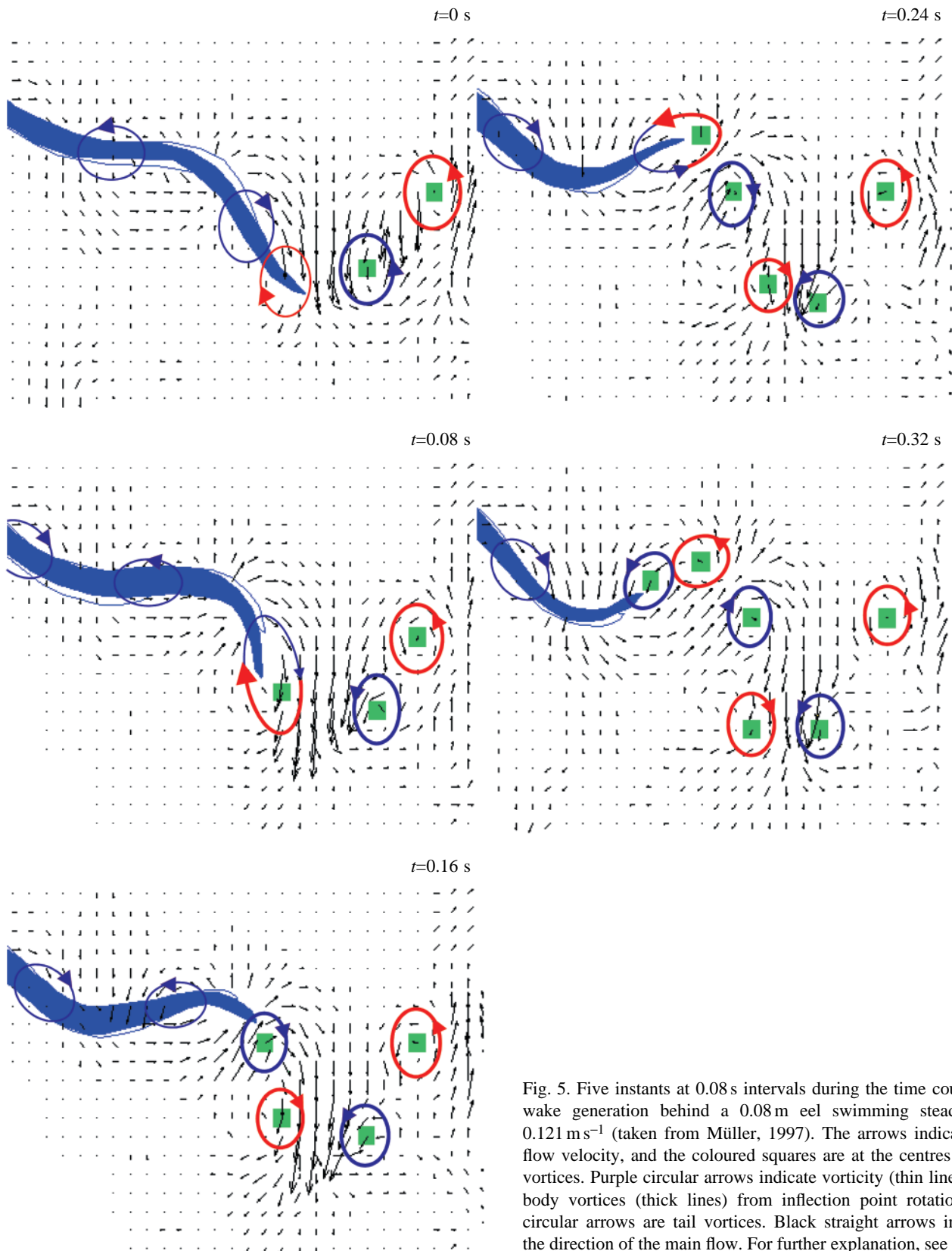


Fig. 5. Five instants at 0.08 s intervals during the time course of wake generation behind a 0.08 m eel swimming steadily at 0.121 m s^{-1} (taken from Müller, 1997). The arrows indicate the flow velocity, and the coloured squares are at the centres of the vortices. Purple circular arrows indicate vorticity (thin lines) and body vortices (thick lines) from inflection point rotation; red circular arrows are tail vortices. Black straight arrows indicate the direction of the main flow. For further explanation, see text.

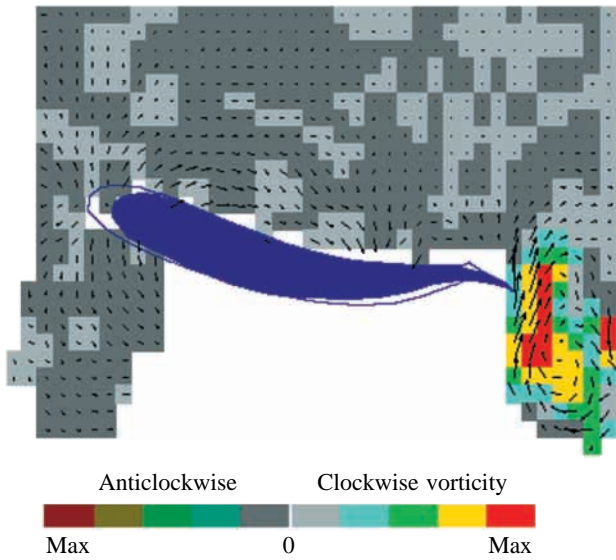


Fig. 6. The flow field adjacent to 0.126 m long mullet swimming steadily at 0.175 m s^{-1} from the right to the left of the field of view. The black arrows indicate the flow velocity. The colours indicate the flow speed (taken from Müller et al., 1997).

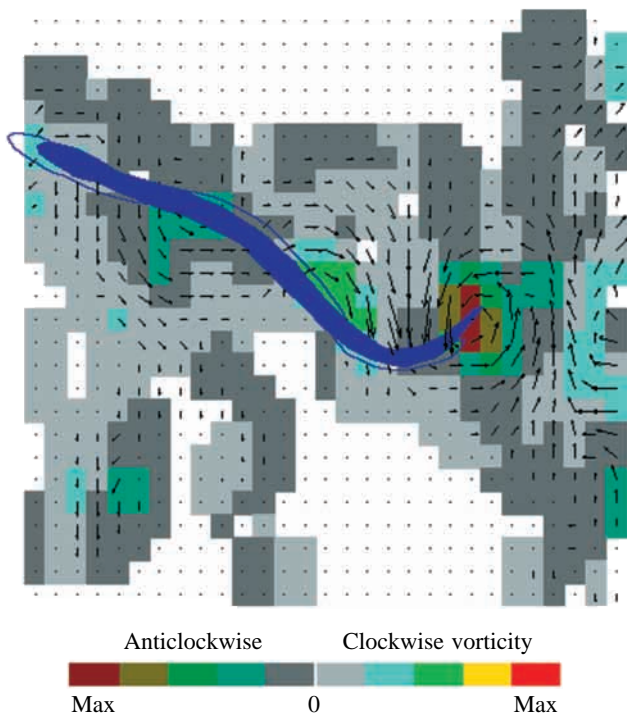


Fig. 7. The flow field adjacent to a 0.08 m long eel swimming steadily at 0.121 m s^{-1} from the lower right to the upper left of the field of view. The black arrows indicate the flow velocity. The colours indicate the level of vorticity in the flow. The downward flow in the lower left of the figure is the remnant of an earlier swimming sequence (taken from Müller, 1997).

clockwise semicircular flow on the contralateral side. Both flows together resemble a clockwise vortical flow pattern separated by the body. Anticlockwise semicircular flows form

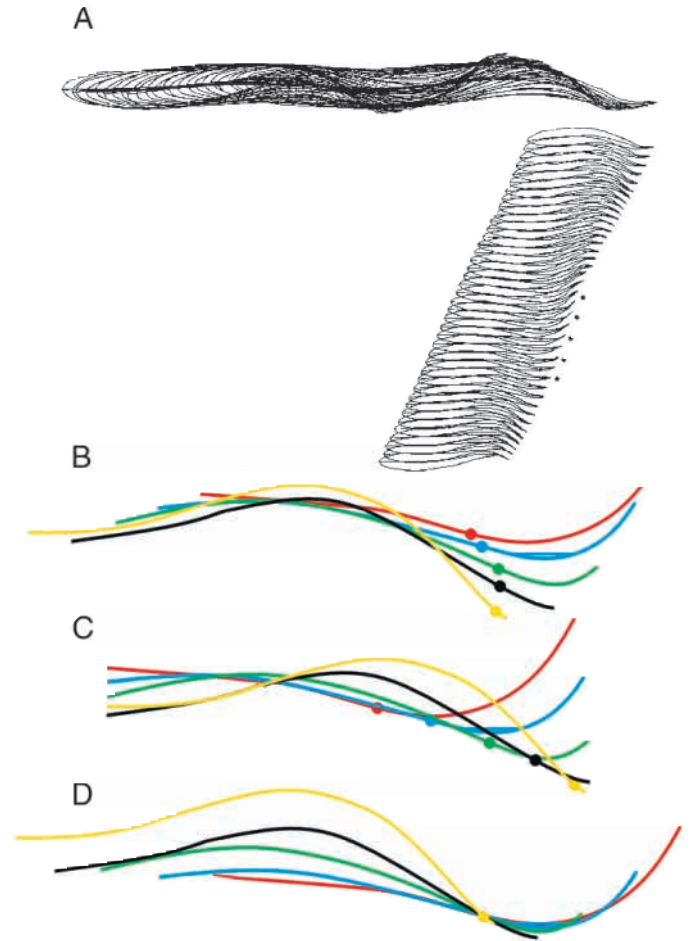


Fig. 8. Inflection points between the concave and convex curvature on a steadily swimming saithe (taken from Videler and Hess, 1984). (A) Digitised film images taken at $100 \text{ frames s}^{-1}$ with computed midlines drawn superimposed (top drawing). On the right, the same images are drawn at half size; the frames used for the analysis in B are indicated by a black dot. (B) Superimposed midlines of the selected frames in an earth-bound frame of reference with the rightmost inflection points drawn as a dot on each centre line. (C) The same lines in a fish-bound frame of reference. (D) The midlines drawn in an inflection-point-bound frame of reference to show the rotation of the body around that point. Note that the vertical axis is twice as big as the horizontal axis in B, C and D for greater clarity.

an equivalent anticlockwise vortical pattern. There are no real vortices because the presence of the body prevents full circulation. These clockwise and anticlockwise proto-vortices alternate along the body. Their centres seem to be at the transition from areas of low to high pressure close to points on the body where the curvature changes from concave to convex or *vice versa*. These points on the body are termed 'inflection points'. In the water, proto-vortices travel down the body in the vicinity of these inflection points. Their strength seems to increase until they are shed into the wake approximately when the inflection point reaches the tail (Müller et al., 1997). No vortices appear to be shed upstream of the tail.

The position and movement of inflection points on swimming fish

Undulations in fish are best studied by determining the midline of the body in dorsal view in a time sequence of film or video frames. A kinematic study of a saithe (*Pollachius virens*) is used to introduce the exact movements of the body. The 35 cm long saithe in Fig. 8A was filmed at 100 frames s^{-1} using a camera in a fixed position (Videler and Hess, 1984). The upper part of the diagram shows the superimposed outlines and the computed midlines of one complete swimming cycle. The same images at half size are shifted laterally over a fixed distance in the diagram to the right. The swimming speed is steady at 1.05 $m s^{-1}$. The midlines of the images indicated with a black dot, representing half a tailbeat cycle, are drawn enlarged in Fig. 8B. The vertical scale in Fig. 8B–D is doubled with respect to the horizontal scale. The rear inflection points on the midline were determined graphically by enlarging each of these lines. The rear inflection point moves down the midline and reaches the tail tip just at the point where the tail is at its leftmost position and starts to move to the right. Fig. 8C shows the same midlines in the fish-bound frame of reference. The inflection points move down the body along a slightly outwardly curved path. Depicting the midline kinematics in an inflection-point frame of reference illustrates the movements of the body relative to the inflection point. The body rotates around the inflection point in a clockwise sense (Fig. 8D). The angle of rotation, and hence the angular velocity, increases over the time course analysed.

The midlines of a 12.6 cm mullet are treated similarly in Fig. 9, which shows half a tailbeat cycle in five equal time intervals. The animal, swimming to the left at 17.5 $cm s^{-1}$, was filmed at 25 images s^{-1} (Müller et al., 1997). The inflection points shown were calculated numerically. The vertical scale of Fig. 9A–C is doubled for greater clarity. The midlines in all three reference systems reveal the same behaviour as the saithe midlines. The inflection point moves along the body away from the mean path of motion and reaches the tail near the point where the tail tip changes direction. The inflection point followed here is on the right-hand side of the mean path of motion. Fig. 9C shows how the midline of the body rotates around the inflection point in an anticlockwise direction with increasing angular velocity.

The same scale adjustment was used to draw the midlines of an eel 8 cm long swimming at 12.1 $cm s^{-1}$ in Fig. 10 (taken from Müller, 1997). In contrast to what is shown by Figs 8 and 9, the rearmost inflection point reaches the tail approximately when the tail tip crosses the mean path of motion. The animal keeps the inflection points fairly close to the mean path of motion while they travel down the body. The rotation of the body around the rearmost inflection point of the first four lines is anticlockwise, and the body rotation around the penultimate inflection point on all five lines is clockwise.

Inflection point kinematics and wake shape

With the inflection point being a good indicator of the centre

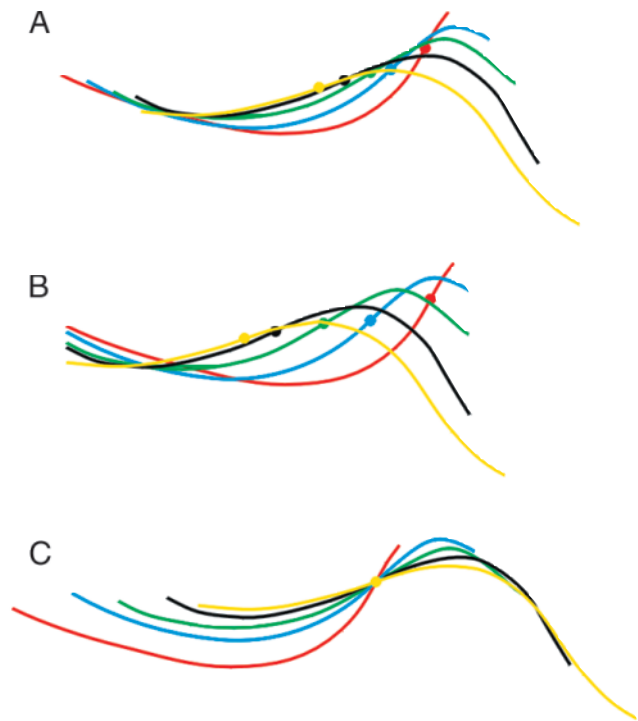


Fig. 9. Numerically calculated inflection points between the concave and convex curvature on a time sequence of five centre lines of a 0.126 m long mullet swimming steadily at 0.175 $m s^{-1}$ (taken from Müller et al., 1997). The sequence covers half a tailbeat cycle. The time between the successive lines is 0.04 s. The midlines are shown in an earth-bound frame of reference (A), a fish-bound frame of reference (B) and an inflection-point-bound frame of reference (C). Note that the vertical scale is twice the horizontal scale.

of the proto-vortex within the spatial resolution of our recordings, we can now relate body kinematics to wake shape. The mullet of Fig. 9 and the eel of Fig. 10 differ in their body wave characteristics in one important point: the moment in the tailbeat cycle when the inflection point reaches the tail tip. In the mullet, the movements of the inflection point and the tailbeat cycle are in phase. Both the inflection point and the tail tip reach maximum lateral excursion at the same instant. This causes the proto-vortex near the inflection point to be shed at the same moment as the stop–start vortex of the tail. We will use the terms ‘tail vortex’ for the vortex shed by the tail when it changes direction and ‘body vortex’ for the proto-vortices shed at the tail. Both the body and the tail vortices in the wake of the mullet have the same sense and merge into one vortex. As a result, one strong vortex is shed per half-tailbeat. The wake behind the steadily swimming mullet analysed in Fig. 9 is shown in Fig. 4 (from Müller et al., 1997). It consists of single vortices to the right and left of an induced undulating jet, as predicted in Fig. 1.

In the eel of Fig. 10, the inflection point and tail tip are out of phase. The inflection point reaches the tail tip half-way through the tail stroke. The consequences of this become obvious in a succession of flow fields (Fig. 5) generated by the eel moving as depicted in Fig. 10. The sequence lasts 0.32 s

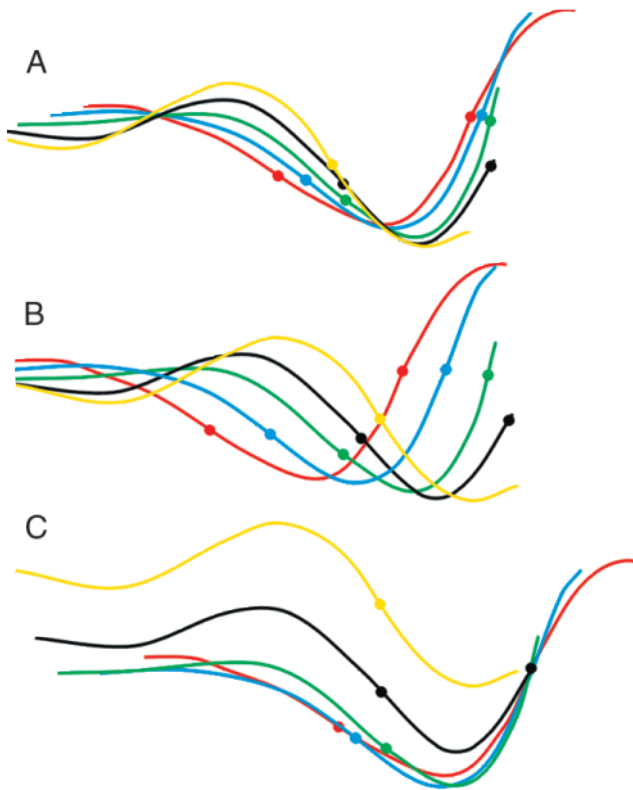


Fig. 10. Midlines of an eel swimming steadily at 0.121 ms^{-1} and calculated inflection points over half a tailbeat cycle in an earth-bound (A), a fish-bound (B) and an inflection-point-bound (C) frame of reference. The vertical scale is twice the horizontal scale for greater clarity (taken from Müller, 1997).

and covers slightly more than one complete tail stroke, starting with the tail tip approaching the point of maximum lateral excursion to the left, followed by a complete half-stroke to the right and ending with the start of the next stroke to the left. Each frame contains the current shape of the eel (in blue) and the shape 0.04 s later (as an outline). The black arrows indicate the flow velocities. The coloured squares code for the discriminant of complex eigenvalues of the velocity vector field, indicating the centres of the vortices (Stamhuis and Videler, 1995). For easier recognition, circular arrows indicate the approximate position of the tail vortices (red) and body vortices (purple), together with their rotational sense. At $t=0$ s, the tail tip is approaching its leftmost position and the clockwise tail vortex (thin red circle at tail tip) is about to be shed. It forms a vortex pair with an anticlockwise body vortex (purple circle) that had previously been shed into the wake. At $t=0.08$ s, a clockwise proto-vortex (thin purple half-circle) has reached the tail tip and is about to be shed next to the tail vortex of the same rotational sense. Before the proto-vortex is shed as a body vortex, it seems to merge with the tail vortex. But soon after, at 0.16 s, it becomes obvious that each of the two vortices has its own centre. At $t=0.24$ s, the tail tip reaches its turning point on the right. An anticlockwise tail vortex is shed into the wake. A proto-vortex of the same sense still remains on the

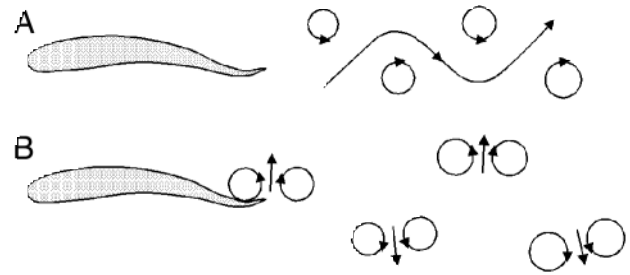


Fig. 11. Schematic representation of the medio-frontal plane of two types of wake behind an undulatory swimmer. (A) The wake consists of two vortices per tailbeat cycle. A jet of water undulates between the vortices and flows in the direction opposite to the swimming direction. (B) Four vortices are shed per tailbeat cycle. Each vortex pair consists of a tail vortex and a body vortex released during the tail stroke (taken from Müller, 1997).

tail, seemingly merging with the tail vortex. At $t=0.32$ s, the final pattern has emerged. Each tail vortex pairs up with the body vortex of the previous half-tailbeat cycle to form a vortex pair. Each vortex pair invokes its own axial jet flow directed obliquely backwards and away from the mean path of motion. The animal is shedding two vortices per half-tailbeat.

Our analysis shows that the wake of an undulating animal in a cross section through the plane of the undulatory movements can take different shapes depending on the instant during a tailbeat cycle when the proto-vortices reach the tail end. Either four or two vortices are shed per complete tailbeat cycle. In the case of four vortices per tailbeat, the tail vortex and the previously shed body vortex rotate in opposite directions and form two pairs, each with an axial jet flow in between. In wakes with two vortices per tailbeat, each vortex contains the combined strength of a tail vortex plus the body vortex delivered at the instant of directional change of the tail. Fig. 11 is a diagrammatic representation of both systems.

Rosen and Gray revisited

Rosen (1959) interpreted the flow behind the danio in the Fig. 3A as reproduced here in Fig. 3B. The vorticity we see is not in a medio-frontal plane through fish and wake, but is situated just underneath the fish. The figure shows the mean path of motion of the fish moving to the right and the track of its tail tip. The wake consists of four vortices per tailbeat. Two strong vortices are shed when the tail tip crosses the mean path of motion during every tailbeat to the left or to the right. The rotational sense of these vortices is clockwise during the stroke to the right and anticlockwise during the stroke to the left. This matches the rotational sense of the body vortices (indicated in blue), and one can assume that this is what they are. The two smaller vortices, each near the position of maximum tail excursion to the right and the left, are probably the tail vortices, shed separately from the body vortices. However, Rosen (1959) indicates a rotational direction opposite to what should be expected for tail vortices. The rotational sense based on our interpretation is indicated in red and green in Fig. 3B.

The picture of the flow around Gray's (1968) eel (Fig. 2) shows clear proto-vortices near the inflection points. Strong vortices are shed at the tail tip, two for every complete tailbeat cycle. This eel, in contrast to that shown in Figs 5 and 10, sheds the body vortices together with the tail vortices. The animal is essentially swimming in the mode used by the mullet in Figs 4 and 9.

Body wakes and body thrust

Body undulations create semicircular flows driven by pressure differences. These flows centre around the inflection points of the body, forming a proto-vortex that is shed at the tail tip. Fish seem to be able to control this process and may choose to let the body vortex enhance the tail vortex or to shed it as a separate vortex at some time during the tailbeat. This body vortex contributes to the wake and hence to the momentum transferred by the fish to the water. The shape of the amplitude envelope of the fish's body waves can influence the amount of rotation and the moment of shedding. If the body vortex merges with the tail vortex, its circulation contributes to the total circulation in the tail vortex and, hence, to thrust. The flow speeds generated along the body can be considerable. In mullet, the flow speeds reached in the proto-vortex at the peduncle are half the flow speed measured just behind the tail (Müller et al., 1997). This suggests that the body can contribute substantially to thrust production.

The function of the wake with four vortices per cycle is not clear. It could be a sign that the fish is not trying to swim efficiently but uses this mode to obtain more dynamic stability. There is no support for this view yet.

This paper demonstrates the two types of wakes caused by undulating bodies and the role of the proto-vortices in the generation of these wakes. It explains how Gray (1968) and Müller (1997) could observe different wakes for an eel. It also explains why the wakes of the eel (Gray, 1968) and mullet (Müller et al., 1997) or the pearl danio (Rosen, 1959) and eel

(Müller, 1997) can be similar despite their obvious differences in body shape and body wave.

We thank Professor R. McNeill Alexander for the encouraging discussion about the interpretation of the strange wake behind the swimming eel. His vast and unambiguous contributions make it a pleasure to teach and work in the field of biomechanics.

References

- Aleyev, Y.G.** (1977). *Nekton*. The Hague: Dr W. Junk b.v.
- Gray, J.** (1968). *Animal Locomotion*. London: Weidenfeld & Nicholson.
- Hertel, H.** (1966). *Structure, Form and Movement*. New York: Van Nostrand-Reinhold.
- Lighthill, M. J.** (1970). How do fishes swim? *Endeavor* **29**, 77–83.
- Lighthill, M. J.** (1975). *Mathematical Biofluid-dynamics*. Philadelphia: SIAM.
- Müller, U. K.** (1997). In the wake of the fish: on the hydrodynamic interactions between swimming fish and water, the effects of ontogenetic stages and swimming kinematics. Thesis, Groningen University.
- Müller, U. K., van den Heuvel, B. L. E., Stamhuis, E. J. and Videler, J. J.** (1997). Fish foot prints: morphology and energetics of the wake behind a continuously swimming mullet (*Chelon labrosus* Risso). *J. Exp. Biol.* **200**, 2893–2906.
- Rosen, M. W.** (1959). Water flow about a swimming fish. *NOTS Technical Publication*. China Lake, CA: U.S. Naval Ordnance Test Station.
- Stamhuis, E. J. and Videler, J. J.** (1995). Quantitative flow analysis around aquatic animals using laser sheet particle image velocimetry. *J. Exp. Biol.* **198**, 283–294.
- Videler, J. J.** (1981). Swimming movements, body structure and propulsion in cod *Gadus morhua*. *Symp. Zool. Soc. Lond.* **48**, 1–27.
- Videler, J. J.** (1993). *Fish Swimming*. London: Chapman & Hall.
- Videler, J. J. and Hess, F.** (1984). Fast continuous swimming of two pelagic predators, saithe (*Pollachius virens*) and mackerel (*Scomber scombrus*): a kinematic analysis. *J. Exp. Biol.* **109**, 209–228.